Temperature Measurements of Single Burning Pulverized Particles

Abdul Salam

Thesis to obtain the Master of Science Degree in

Energy Engineering and Management

Supervisor: Prof. Mário Manuel Gonçalves da Costa

Examination Committee

Chairperson: Prof. Francisco Manuel da Silva Lemos

Supervisor: Prof. Mário Manuel Gonçalves da Costa

Member of the Committee: Prof. Sandrina Batista Pereira

June 2018

ACKNOWLEDGEMENTS

I would like to thank my supervisor, Prof. **Mário Manuel Gonçalves da Costa** for the support, guidance, availability and teachings given during the elaboration of this master's thesis.

I also want to thank **Sandrina Batista Pereira** for her cooperation and for the help given during the experimental work, data analysis and writing of the dissertation.

I also want to thank **Manuel Pratas, Tomás Prudente**, for always being present in the lab for any assistance and all other colleagues and friends from the laboratory, for the good times spent and support given during this work.

I would like to thank all the people I met during the development of this dissertation, and who somehow contributed to its elaboration.

Finally, I would like to thank my family, my friends for their support, patience and understanding throughout my academic years.

ABSTRACT

The main aim of this work is to measure the temperature of single particles of coal and biomass burning in air using a two-color pyrometer. A Brazilian bituminous coal with particles size below 150 μm and a Portuguese wheat straw with particles size in the range 150-200 μm were used as fuels. The combustion took place in an electrically heated drop tube furnace with a wall temperature of 1373 K. The drop tube furnace was fitted with a central, transparent, 82 cm long quartz tube with an internal diameter of 6 cm. The single solid fuel particles were injected from the top of the drop tube furnace with the help of a syringe needle. A two-color pyrometer was used to measure the particle temperature. The device was placed perpendicular to the direction of the flow. The particle temperature was measured along the drop tube furnace in order to obtain axial profiles. The present method produced satisfactory results that are in agreement with previous studies.

Keywords: Drop tube furnace, two-color pyrometry, single particle temperature

Contents

List of Figures

List of Tables

Nomenclature

Acronyms

2C	Two-color
CCD	Charge-coupled device
DTF	Drop tube furnace
FC	Fixed carbon
GHG	Greenhouse gases
ID	Internal diameter
LHV	Lower heating value
MPT	Mean particle temperature
TGA	Thermogravimetric analysis
VM	Volatile matter
WWP	White wood pellet

Greek letters

α	Absorption rate
ϵ	Emissivity
ρ	Reflection rate
σ	Stefan–Boltzmann constant
τ	Transmission rate
Λ	Wavelength

1. INTRODUCTION

1.1. Motivation

The demand of energy is on the rise from last few decades since the industrialization and urbanization has increased dramatically. The global primary energy consumption (in Mtoe) has increased by 53% from 1995 to 2015 [1]. A lot of successful efforts are being done by improving the energy efficiency and advancements in available technologies to hinder this growth, which can be reflected from the fact that the rate of primary energy consumption has slowed down in recent years, being only 1.1% in 2014 and 1% in 2015 [2]. But it is still expected that the energy consumption will increase by 31% from 2015 to 2035 [1].

Fossil fuels have been the foremost important source of energy and will remain so because the energy generated by renewable sources is still insufficient to keep up with the growing energy consumption rate. Coal is still the most abundantly used fossil fuel in power plants on world scale. Although, the use of fossil fuels has decreased (4% in production and 1.5% in consumption in 2015), they are still considered to be the most stable, cheap and abundant source of energy in the whole world [2]. Coal still has the highest reserves-to-production ratio as compared to other fossil fuels and it is said to have enough stocks available to power the world for the next 114 years [2].

There are also a lot of concerns related to the burning of fossil fuels due to the emission of pollutants. Currently, the major concern of using the fossil fuels is to minimize their environmental effects. The main pollutant gas species emitted to the environment from the combustion of fossils are CO_2, CO, NOx, SOx and particulate matter. Although CO_2 is essential for the photosynthesis process, its excess release in the ambient is responsible for the greenhouse effect and ultimately global warming. The CO_2 emitted by burning the fossil fuels increased by 0.1% in 2015 alone [2].

To overcome these environmental concerns, a lot of efforts are being done to minimize the pollutants such as co-firing of biomass with coal (see Figure 1) or use of biofuels. This is done not only to reduce pollution but also to decrease the dependency on imported fossil fuels and increase employability [3]. One of the main renewable sources is biomass that has a great potential to be used in future to minimize gas pollutants. One of the biggest reason of its great potential is its neutrality of CO_2 emissions, which means that the CO_2 emitted during its combustion cannot be more than its consumption during photosynthesis. This is the reason why it can play a key role not only just to fulfill global energy demand but also to cater the industrial and agricultural waste and improve the social and economic aspect of the community.

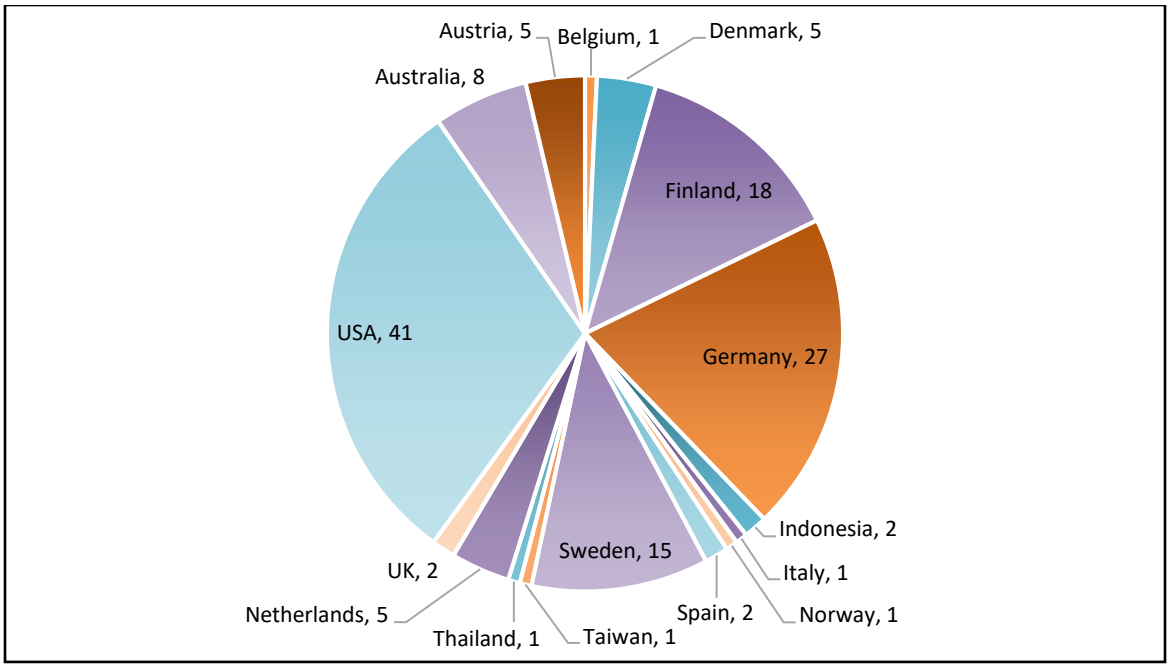

Figure 1: Geographic distribution of power plants that have experienced co-firing of biomass with coal [4]**.**

A recent investigation by Haykiri et al. [5] revealed that coal/biomass blends can be used to utilize the excess heat generated by oxy-fuel combustion of coal. They used a TGA-DSC technique at 1173 K to burn mixtures of a lignite coal and two biomass fuels, at high oxygen partial pressures. It was found that heat flux during burning of lignite was increased dramatically when the dry air in the oxidizing medium was replaced with neat oxygen. However, in case of co-firing of lignite with biomass, this excess heat flux was reduced when the oxidizing medium was replaced and thus, the temperature of the combustion chamber was controlled. So, it was concluded that co-firing of coal/biomass in enriched oxygen environments can be an alternative to recycling of CO_2 in future oxy-fuel systems.

Although co-firing biomass can be really useful, it is still a novel technology and a lot of technical aspects need to be worked upon as coal and biomass have different burning characteristics, ignition times and temperatures. Therefore, knowledge of technical and economic aspects is mandatory as it will directly affect the combustion process, furnace shape and size, efficiency and ultimately the cost.

Among all the parameters needed for fuel combustion, temperature is the most important parameter in all the combustion processes because every part of a combustion process such as devolatilization, ignition and burnout are related to it. Therefore, it is always a center of interest for researchers to measure the particle temperature of fuel during combustion, either surface temperature or inside the particle. Few important reasons for such extensive research on temperature, as stated by Joutsenoja et al. [6], are as follows:

a) The kinetics of carbon residue oxidation depends strongly on particle temperature, so its measurement constitutes the key element for the determination of combustion reaction rates.
b) Particle temperature is the most important parameter in the calculation of heat flow to/from the particle, both by convection, as well as by radiation.
c) It can also play a detrimental role in the identification of problems appearing during coal utilization, such as fly ash formation and slagging, and its deposition on the boiler walls.

There are a lot of studies regarding the combustion profiles, ignition and delay times, effects of oxy-fuel conditions on combustion process but there is a gap in literature regarding the temperature of single fuel particle of coal or biomass when burning in air. So, in this context, this work is focused on estimating the single particle temperature of coal and biomass burning in air.

1.2. Previous studies

In recent years, biomass has gained a massive interest in co-firing it in coal-based power plants with just minor modifications in the design rather than building a new biomass-specific power plant. Usually biomass has lower heating value and less carbon but higher volatile content and oxygen as compared to coal [7]. So, biomass has been the center of interest from past few years and a lot of research is going on.

Fuel burning profile is an important factor in co-firing biomass and coal as it directly affects the design of the combustion chamber and ultimately the cost. Hence fuel particle temperature, being the most important aspect of the burning profile, comes out as the center of interest for many researchers.

Khatami et al. [8] assessed the combustion behavior of single fuel particles burning in different environments such as O_2/N_2 and O_2/CO_2 , with oxygen mole fractions ranging from 20-100%. Four pulverized coals from different ranks (a high-volatile bituminous, a sub-bituminous and two lignites) as well as a biomass residue (pulverized sugarcane-bagasse) were used. High oxygen mole fractions in N_2 was also employed for comparison purposes. All the solid fuels were burned in a laboratory scale, electrically heated, vertical drop tube furnace with a fitted quartz tube. Single particle combustion was observed by using a 3-color pyrometer and high-speed cinematography simultaneously.

The drop tube furnace with a radiation cavity, 25 cm long, was heated up to 1400 K by hanging molybdenum disilicide elements. The gas mixtures were introduced from a water-jacketed stainless-steel injector equipped with a flow straightener into a transparent quartz-tube having ID of 7 cm. The particles were introduced through a port at the top of the nozzle by a syringe-needle system to ensure single particle entry. The gas temperature profiles of all the gas mixtures were also measured by suction thermometry along the centerline of quartz tube. With replacement of N_2 with CO_2 and increasing percentage of O_2, all fuels tended to burn in one-mode (simultaneous volatile and char combustion) while

it turned to be two-mode behavior when the coal rank was increased from lignite to bituminous. The temperature and the burnout times of coal, for one-mode combustion, were found to be in between the volatile and char (two-mode) temperatures and burnout times of similar particles under similar conditions. Moreover, particle burnout temperature and luminosity were increased, and burnout time was decreased with increasing O_2 concentration.

Levendis et al. [9] studied the combustion behavior of four different pulverized biomasses which included sugar cane bagasse, pine sawdust, torrefied pine sawdust and olive residue. Single particles of these solid fuels were burned in a DTF at 1400 K, in both air and O_2/CO_2 atmospheres containing 21, 30, 35 and 50% oxygen mole fractions. High-speed camera and a pyrometer were also used for temperature-time histories. Results showed that all the fuels burned in two-phases. In the first phase, volatiles were evolved and burned in a spherical envelope flame with low luminosity. In the second phase, char residues were ignited and burned with brief time periods. Moreover, changing from air to oxy-fuel atmosphere, intensity of combustion was impaired, combustion temperatures were reduced, and burnout times were increased at 21% O_2 mole fraction. Increasing the mole fraction of O_2 from 28-35% restored the combustion intensity of single biomass particles.

Milena et al. [10] also studied the effect of oxy-fuel conditions on coal char particles in a DTF using a high-speed camera and two-color pyrometer. Particles sizes used were 100-125 μm and 180-200 μm at three different temperatures. The results were in agreement with the previous study of khatami et al. [8] that increasing the O_2 concentration increased the particle temperature and decreased the burnout duration and the effect was reversed in case of CO_2.

Timothy et al. [11] measured the burning history of a single coal particle using a two-color pyrometer. Two lignite and three bituminous coal particles ranging from 38-45 μm and 90-105 μm were used at furnace temperature of 1250 K and 1700 K in atmosphere containing 15-100% oxygen. The apparatus had an astro model furnace with a two-stage feeding system together with a top-mounted pyrometer to get the particle radiations against the dark background. The model was developed to simulate the combustion of coal particles. Results showed that the burning temperature and effect of O_2 increment were in agreement with values predicted by the model till 3000 K (50% O_2) but the further increase in O_2 resulted in overprediction of temperature.

Maloney et al. [12] also measured the changes in the particle temperature and size during the early stages of heating and devolatilization using a radiation source and a single wavelength pyrometer. It was found out that the measured values exceeded the predicted model values (over 50 percent) owing to the uncertainty in assigning the thermodynamic and heat transfer properties as well as particle shape factors.

Bejarano et al. [13] investigated the combustion behavior of the single particles of bituminous and lignite coal as well as the spherical and monodisperse synthetic chars at increasing O_2 mole fraction in N_2 and CO_2 environments. The experimental setup had a DTF at temperatures of 1400 K and 1600 K and the

particle temperature was measured by three-color pyrometer. It was found out that coal particles burned at higher mean temperatures and shorter combustion times in O_2/N_2 than in O_2/CO_2 environment keeping the same O_2 mole fraction in both. Similarly, bituminous coal volatile and char temperatures comparable to air (21% O_2) were obtained in CO_2 atmosphere when the oxygen content was 30%.

Riaza and Levendis [14] conducted another investigation involving four different coal ranks; anthracite, semi-anthracite, medium-volatile bituminous and high-volatile bituminous coal. The experimental setup had an electrically heated DTF at 1400 K, three-color pyrometer and a high-speed high-resolution camera. The combustion environments used were air (21% O_2/79% N_2) and four different oxy-fuel conditions: (21% O_2/79% CO_2), (30% O_2/70% CO_2), (35% O_2/65% CO_2), (50% O_2/50% CO_2). It was deduced that the ignition temperatures increased with the increasing coal ranks and decreased with the increasing oxygen concentration. Secondly, replacement of N_2 with CO_2 (changing from air to oxy-fuel condition) impaired the combustion intensity but increasing the oxygen concentration to 35%, restored its intensity.

1.3. Objectives

The objective of this study is to measure the temperature of single particles of coal and biomass in air using a two-color pyrometer. The solid fuels were burned in an electrically heated drop tube furnace at a wall temperature of 1373 K. For each solid fuel, particle temperature measurements were taken along the drop tube furnace in order to have axial profiles of the temperature history of each solid fuel.

1.4. Thesis outline

This thesis is divided in five chapters, of which this constitutes the introduction. This chapter includes the literature survey, the objectives of the study and the outline of the thesis. Chapter 2 presents the fundamentals of the pyrometry and solid fuels combustion and chapter 3 presents the materials and methods used in this work. Subsequently, chapter 4 presents and discusses the results obtained in this work and, finally, chapter 5 summarizes the main conclusions and lists some suggestions for future research.

2. FUNDAMENTALS

2.1. Solid fuels combustion

Solid fuels such as coal and biomass are organic fuels. Upon heating, the organic part is pyrolyzed which is released then as volatile matter. The remaining part containing carbon and mineral matter is referred as Char [15]. The combustion process of solid fuels can be represented by four main steps [16].

- Heating and drying phase
- Devolatilization and ignition
- Volatiles combustion
- Char oxidation

Figure 2 shows the steps involved in combustion process of solid fuels. The last two steps can also overlap in few cases due to very high heating rates.

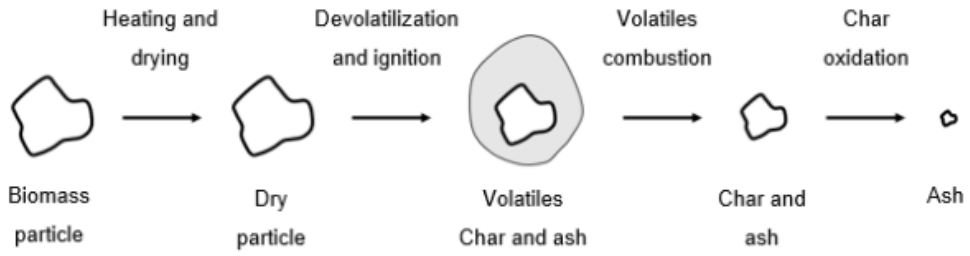

Figure 2: Schematics of combustion process of solid fuel particle [17]**.**

Devolatilization and volatile combustion

The release of volatile matter due to burning of solid fuel is known as devolatilization. During this step, moisture level is decreased as the temperature rises. On further increasing the temperature, gases and heavy tarry substances are emitted. In case of coal, this content can make up from few percent up to 70-80% of the total coal weight, depending on the coal type and the burning conditions. Depending upon the particle shape, size and temperature, this step can take few milliseconds to several minutes. They react with oxygen in the vicinity to produce bright diffusion flames [15].

Char combustion

The residual char particles mainly contain the mineral matter, carbon, surplus nitrogen and some amount of sulfur. These particles have some cracks due to the release of gases and heat stress. The characteristics of char depend on the type and size of solid fuel as well as the heating conditions.

Char combustion is a heterogenous gas-solid reaction because the oxygen diffuses into the char porous particle and reacting to pore surface. This step is usually much slower than devolatilization step, requires millisecond to several minutes depending on the coal size, shape, temperature, pressure and oxidizer concentration.

A summary of the primary reactions occurring during this step is shown in Table 1.

Reactions	**Heat of Reaction (KJ)**
$C + O_2 = CO_2$	-392.9
$C + ½ O_2 = CO$	-111.2
$CO + ½ O_2 = CO_2$	-281.7
$C + CO_2 = 2CO$	+170.5

Table 1: Primary reactions during char combustion [15]**.**

2.1.1. Coal characterization

Coal is formed by the decomposition of combustible organic material, mineral matter and moisture such as decomposition of plants remains under high temperature and pressure during the course of millions of years. Since coal-forming time can be different so many coal forms exist such as Lignite which is the youngest of all the coals, brown to black in color, with relatively higher volatile and moisture content. It also has higher ash content and therefore, lower heating value. The next rank is the Sub-bituminous coal which is black like bituminous. It has lower moisture content compared to lignite but still, more than bituminous so its heating value is also less than bituminous. The next rank is the bituminous which has lower moisture content and the volatile content ranging from high to medium. It is easy to ignite and burn out and its heating value is high. Anthracite has the longest coalification age and the oldest of all coals. It is jet black, hard and brittle in nature. It has lowest moisture content and highest heating value and carbon content. But it is difficult to ignite and burn out [15].

2.1.2. Biomass characterization

Biomass can be defined as any solid biodegradable organic material that can be combusted and

used as fuel. It can be classified according to its source and origin into the following groups [18]:

- Wood (oak, pine, beech, etc.) and woody biomass (branches, bushes, leaves, etc.).
- Herbaceous and agricultural biomass (grasses, straws, husks, shells, etc.).
- Aquatic biomass (microalgae, seaweed, sweet-water weeds, etc.).
- Animal and human biomass wastes (bones, chicken litter, etc.).

- Contaminated biomass and industrial biomass wastes (municipal solid waste, sewage sludge, etc.).
- Biomass mixture.

The biomass is very heterogenous owing to its origin as it is constituted by variable elements of organic and inorganic compound. Generally, the main elements that constitute the organic part are Carbon, Oxygen, Hydrogen and Nitrogen and the inorganic part, usually known as the ash-forming part, are formed by Silicon, Calcium, Potassium, Magnesium, Sodium, Iron, Chlorine, Phosphorus and Aluminum [18].

The organic portion of the biomass consists of three constituents which are cellulose, hemicellulose and lignin. Their composition on weight basis on dry basis is largely dependent on the type of biomass but roughly, its 40-60% cellulose, 20-40% hemicellulose and 15-25% lignin [19][20].

Hemicellulose consists of a mixture of heterogeneously branched polysaccharides composed of sugars such as xylose and other five carbon monosaccharides. It has an amorphous and irregular structure with easily degradable branches [20]. The other constituent cellulose is a strong non-branched structure consisting of a long glucose polymer and a high thermal stability with the release of volatiles [20]. Third constituent which is lignin has an amorphous structure made of aromatic rings with several branches whose proportion varies according to the origin of the biomass. The chemical bonds present within its molecules are degraded for a wide range of temperatures [21][20].

Table 2 shows the general composition of some biomass types compared with coal.

Proximate analysis of some biomass feedstocks (wt%)

Biomass	Moisture[a] (%)	VM (%)	FC (%)	Ash (%)	LHV (MJ/kg)
Wood	20	82	17	1	18.6
Wheat straw	16	59	21	4	17.3
Barley straw	30	46	18	6	16.1
Lignite	34	29	31	6	26.8
Bituminous coal	11	35	45	9	34

[a] Intrinsic.

Table 2: Proximate analysis of biomass and coal (wt.%) [21].

2.2. Fundamentals of pyrometry

There are two common techniques for measuring the temperature [22]:

- Contact method
- Non-contact method

Contact methods usually use thermocouples that can be used either by immersing in the fluid, or by directly touching the solid surface. Sometimes, it is nearly impossible to use this method in laboratory or industry because the object is either inaccessible, moving or changing its phase. These phenomena can occur in case of combustion of coal particles, so that's why non-contact methods are employed for such process that make use of optical pyrometers [22].

The word pyrometer comes from the Greek word "pyro" that means *fire;* and "meter" that means *to measure.* The word pyrometer was originally coined for a device capable of measuring the temperature of an object by its *incandescence.* Pyrometers measure the temperature of the objects without touching them, but the question arises how?

Every object whose temperature is above absolute zero (-273 ̊C) emits radiations, which depend on the object temperature. Commonly the word infrared radiation is used because most of the radiations emitted by these objects lie in the electro-magnetic spectrum, which is above the red light, also known as infrared region (see Figure 3).

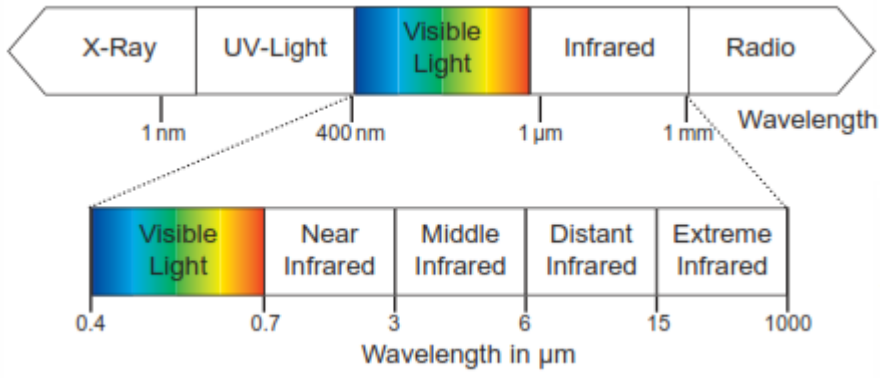

Figure 3: Electro-magnetic spectrum [23]**.**

Like radio broadcasting where the energy emitted by the transmitter is captured by the receiver and then converted into sound waves, the emitted heat radiation from a hot object is captured by the detector and then converted into an electric signal. Figure 4 shows a typical non-contact modern pyrometer which is used for such measurements.

Figure 4: Modern pyrometer [24]**.**

2.2.1. Basic laws of pyrometry

In the field of pyrometry, the basic laws presented by Max Planck (1858-1947), Wilhelm Wien (1864-1928), Josef Stefan (1835-1893) and Ludwig Boltzmann (1844-1906) are used as the foundation [23]. *Planck's law* describes the intensity in the wavelength interval dλ:

$$dM = C_1 \frac{1}{\lambda^5} . \frac{1}{e^{C_2/\lambda T - 1}} d\lambda \quad (1)$$

where C_1 and C_2 are radiation constants and $C_1 = 3.74 * 10^{-16}$ W/m^2 and $C_2 = 1.44*10^{-2}$ mK.

Similarly, *Boltzman law* describes the temperature dependency of the radiated intensity of the total wavelength range:

$$M = \sigma T^4 \quad (2)$$

where $\sigma = 5.67*10^{-8}$ W/m^2.K^4

The *Wien's law* describes the relation between the wavelength and the temperature whereby this wavelength shows the maximum radiation intensity:

$$\lambda max = \frac{C_3}{T} \quad (3)$$

where $C_3 = 2.898*10^{-3}$ mK.

It should be noted that all these laws are applied on black bodies; the bodies which absorb 100% of all the radiations falling on them in all the wavelengths.

Properties of real objects

When an incident ray of light falls on a reflecting surface such as mirror, different phenomena happen depending on the nature of the object such as reflection, transmission and absorption (see Figure 5). In pyrometric measurements, emissivity is one of the most important factor that plays a key role in accuracy of measurements. The emissivity of the object may vary depending on its nature such as it can be either grey body or real radiation body. To understand these concepts, we need to understand these properties of objects which are shown in Figure 5 [23].

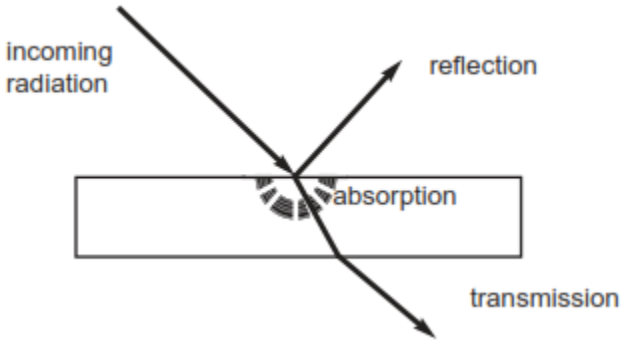

Figure 5: Different light scattering phenomenon [23]**.**

When a large part of incident rays is reflected off a bright, smooth boundary between different mediums, it is called reflection. There can be *focused reflection*, such as from a mirror or lacquered surface. Other than that, there can be *diffused reflection* from rough surfaces such as paper. It is usually represented as reflection rate ρ. Another phenomenon that can occur is absorption in which some parts of the incident rays can be absorbed by rough and dark surfaces and it can happen across a wide or narrow band spectrum. For example, a red car appears red because it absorbs all the colors. It is usually represented as absorption rate α. When a certain part of incident light is penetrated through the object and passes through it, it is called transmission. It usually happens from transparent materials and can be selective as well. For example, a normal glass transmits the entire spectrum of visible light while tinted glass allows only a certain part of spectrum. It is represented as transmission rate τ.

The values for τ, α, ρ are always in between 0 and 1 and their total sum is always 1.

$$\tau + \alpha + \rho = 1 \tag{4}$$

As in case of fuels, the solid fuel particles absorb and emit the radiations which are then analyzed by pyrometer. So, depending on the nature of absorption, they can further be classified into grey and real

radiation bodies. These concepts are established by defining an ideal black body that absorbs all the radiations falling on it. So, in this case absorption coefficient $\boldsymbol{\alpha = 1}$ and $\boldsymbol{\tau}$ and $\boldsymbol{\rho}$ will be zero. In thermal equilibrium, a body which absorbs well emits well. (Robert Kirchhoff, 1824-1877). This means that its absorption coefficient $\boldsymbol{\alpha}$ equals its emission coefficient $\boldsymbol{\epsilon}$ [23]. So, in this case

$$\epsilon = \alpha \tag{5}$$

Emissivity coefficient is the ratio of emission output of an object to the emission output of a black body radiation source at same temperature. Its value is always less than 1 because ideal black body doesn't exist. So, for real conditions, the grey body is defined whose emissivity remains constant within a certain spectrum range. It appears grey because in visible light, it reflects all the colors of light evenly. Another important term used is the real radiation body whose emissions do not match with black or grey body. Figure 6 shows all the different types of bodies depending on the nature of radiations.

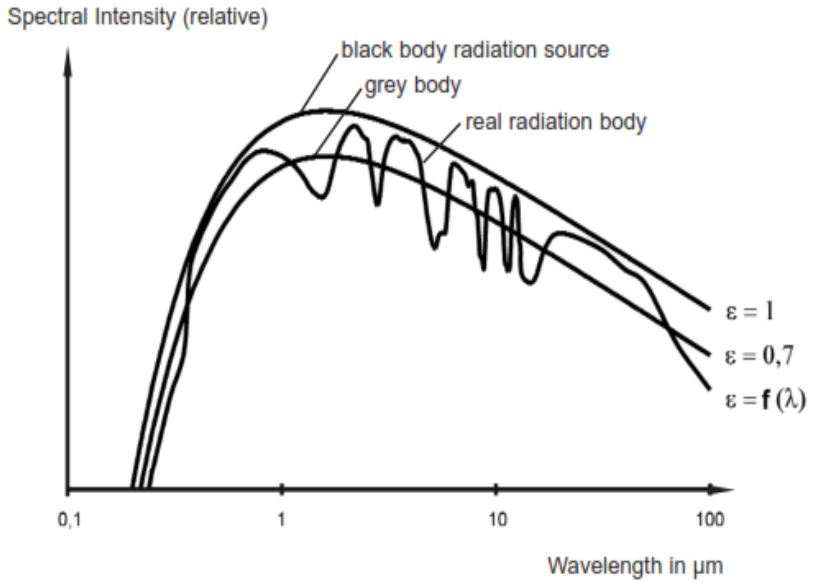

Figure 6: Types of radiation emitting bodies [23]**.**

Having discussed the fundamental concepts of pyrometry, here is the basic working principle and main construction parts. Construction of almost all the pyrometers is the same with few differences depending on their types and is shown is Figure 7.

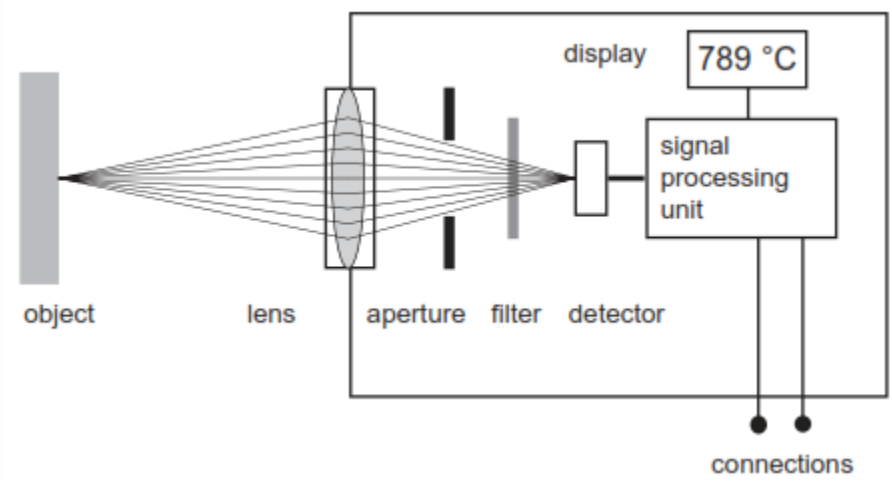

Figure 7: Construction of a pyrometer [23]**.**

The main parts of a pyrometer are lens, aperture, filter, detector and a signal processing unit. The infrared radiations emitted by the object, which is under consideration, are directed on to the lens and then passed on to the aperture that blocks the unwanted radiations from its edges. The function of the filter is to allow only the desired spectral range which falls on the detector thereby converting it into an electrical signal. The final part is the signal processing unit that linearizes the signals and changes them to standard output signal which can be then read on display [23].

2.2.2. Types of pyrometer

There are following pyrometric technologies available at present:

1. Short-wavelength pyrometers have wavelengths usually less than 3 μm. In comparison with the long-wavelength pyrometers, errors are smaller for moderate emissivity variations, misalignment and optical obstructions.
2. Long-wavelength pyrometers typically operate in between 8-14 μm. They can be ideal to operate in low temperatures (below 100 ̊C) and high emissivity materials but a small variation in emissivity can result in large temperature errors.
3. Two-color pyrometers are the type of ratio pyrometers that use two different wavelengths and then calculate the ratio from the signals thereby measuring the object temperature. One advantage of this type is that when the signals are measured by different narrow segments of spectrum or wavelengths, theoretically emissivity is same at each wavelength thereby the effect of emissivity cancels out in temperature measurements and it can be removed from mathematical equations [25].

Figure 8 shows the phenomenon of radiation interference and the processing of ratio pyrometer in such circumstances. Let's take an example of a pyrometer with the wavelengths of 0.95 µm and 1.05 µm. S1 and S2 represent the signal strength of radiations emitted by the object. The output signal, which will be the ratio of S1 and S2, will not be affected even if the fuel particle does not fill the spot size or if there is an interference of smoke or suspended matter which is 50% in this case. It can be seen that the signal ratio before and after the interference remains same.

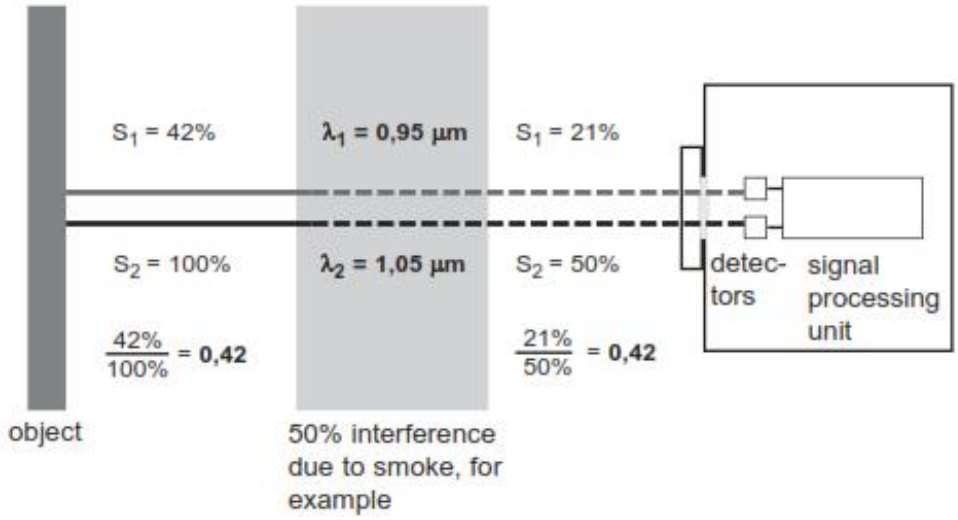

Figure 8: Two-color pyrometer [23].

4. Multi-wavelength pyrometers are used where emissivity is low and is changing with the process. These pyrometers use 3 or more wavelength bands and can detect minor variations in emissivity and go through a "learning" process to adapt to different emissivities.

2.2.3. Advantages of pyrometer

The main advantages of pyrometer over contact devices are as follows [23]:

1. The pyrometer takes a very short response time. In case of contact measuring devices, a probe is used to measure the temperature by physically touching the object and thus it takes time to give the signal as the probe needs to be at the same temperature as the object that involves conduction. Therefore, it takes longer response time. Contrary to this, pyrometer measures the radiation signal and produces an instant temperature value in fraction of seconds.

2. Pyrometers use a portion of radiation signals that are emitted from the object, so they don't influence the temperature of the object while in case of contact thermometers, the device must touch the object and reach at its temperature. In doing so, it can cause heat loss of the object thereby influencing the object's temperature at contact point. In case of materials, non-contact devices cannot be damaged in

the same way as contact thermometers or thermocouples. So, it's obvious that non-contact devices have relatively longer life span than contact devices due to protection from wear and tear.

3. Pyrometers are capable to measure moving object's temperature quite effectively because of their quick response time. In case of contact devices, they can cause scratching on object's surface, but non-contact devices are safe to use in such situations. Also, no drilling or fastening is required to measure the temperature in case of non-contact devices.

4. The optics of pyrometer can easily be adjusted to measure the temperature of small objects**.** It's possible to measure the temperature of bodies with diameter of 0.2 mm for example thin wires which may induce a great error if measured by contact devices. Similarly, very high temperatures can also be measured easily with pyrometers as there is no direct contact. For example, NiCr-Ni thermocouples can measure up to a temperature of 1300 ℃ after which they change physically. Practical example is the temperature of forging steel.

It can also measure the temperature for inaccessible bodies. Pyrometers, due to their compact design, can be installed nearly anywhere if they have a clear line of sight with the object. For example, temperature measurement inside furnaces. Objects that are electrical conductors can also be measured without any danger of short-circuiting or danger to the user. For example, temperature measurement of electric terminals in switch boxes.

2.2.4. Uncertainties in measurements

There are possibilities of different types of errors/uncertainties in pyrometric readings that can be originated in following ways [22].

1. Errors can originate by radiation interference with furnace gas due to the space in between the pyrometer and the burning particle as it contains gases like oxygen, nitrogen, carbon dioxide and water vapor. These gases absorb some of the radiation spectrum from the particle and hence effect the pyrometer reading. It can be minimized by considering the absorption band of these gases and selecting the respective wavelength bands.
2. Errors can also originate by the background radiations. These kinds of errors generate from different sources such as direct radiations from the furnace walls, radiation from the furnace walls reflected from the inner surface of injector, radiations from the walls reflected on the particle surface as well as the radiations from room lightening. Some of these can be avoided by design of injector and better light collection system of pyrometer.
3. Errors may generate by assuming the coal particles to be grey body (emissivity independent of wavelength). Usually emissivity depends on the material properties such as temperature, roughness, shape and wavelength of observation. Fletcher and coworkers [26] worked on the

spectral and total emissivity of coal ranks ranging from lignite to bituminous within a temperature range of 400-473 K. Their particle size ranged from to 40 to 120 μm and the data was collected at wavelengths in between 2.2 and 17 μm. It was observed that with the higher coal ranks, they behaved more like grey bodies. It was also concluded that with the decrease in wavelength of observation, and increase in the particle size, coal rank and extent of burnout, the coals behaved increasingly as grey bodies. However, as the burnout increased, the particle emissivity may either increase, decrease or remain constant depending on the region of wavelength spectrum being considered. Such uncertainties in the emissivity may have a significant effect on the particle temperature measured by multi-color pyrometers.

4. Some errors stem from numerical computations and statistical procedures e.g. method of choosing the base-line signals and linear or non-linear fittings.

3. MATERIALS AND METHODS

This chapter describes the materials and methods used in this research.

3.1. Solid fuels

The solid fuels used in this work include a Brazilian bituminous coal with a particle size below 150 μm and a Portuguese wheat straw with a particle size in the range of 150-200 μm which are shown in Figure 9.

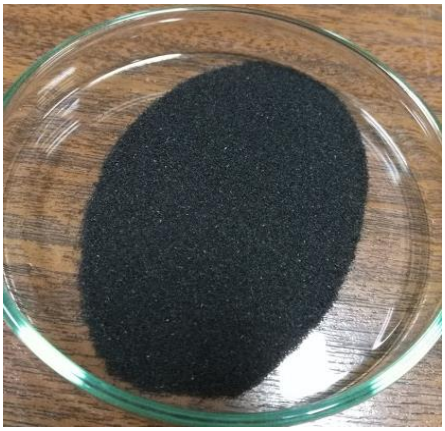

Bituminous coal

Wheat Straw

Figure 9: Solid fuels used in experiments.

Table 3 shows the main properties of the both solid fuels.

		Wheat straw	Brazilian coal
Proximate analysis (wt.%, as received)	**Volatiles**	64.9	27.8
	Fixed carbon	12.4	38.5
	Ash	14.7	33.7
	Moisture	8.0	5.3
Ultimate analysis (wt.%, dry ash free)	**Carbon**	41.1	50.8
	Hydrogen	5.3	3.8
	Nitrogen	0.7	0.9
	Sulfur	<0.2	0.9
	Oxygen	52.6	9.8

Table 3: Properties of solid fuels [27][28].

3.2. Drop tube furnace

Figure 10 shows the schematics of the DTF and all the auxiliaries. This DTF is suitable for the present experiments since it has a relatively simple configuration and can reproduce the conditions encountered in practical systems. The combustion studies of pulverized coal and biomass were carried out in this electrically heated, vertical DTF at a wall temperature of 1100 ℃ that was continuously monitored by two type-S thermocouples. The DTF has two opposed rectangular quartz windows with 2 cm width and 20 cm height for viewing. The DTF is fitted with a cylindrical quartz tube with a length of 1 m and an inner diameter of 66 mm. The radiation cavity of DTF is 30 cm long. The feeding unit (see Figure 11) consists of a nozzle to inject the solid fuel particles with the help of a syringe and a rotameter to measure the air flow rate. The fuel particles, stored in the syringe, are injected in the water-cooled injector by gravitational force. Gentle pushes and rotation of the syringe help to inject the single particles of fuel inside the injector without clogging.

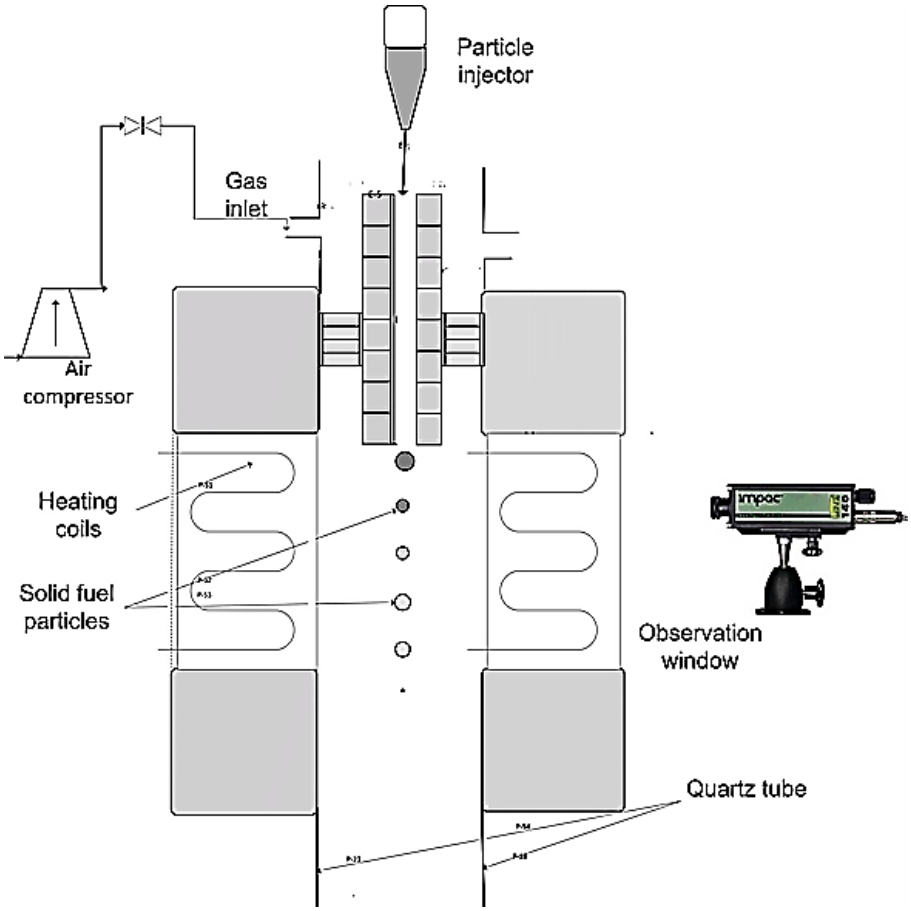

Figure 10: Schematics of drop tube furnace**.**

Figure 11: Injector with air and water supplies.

The temperature measurements of the solid fuel particles were performed with a two-color pyrometer, which was aligned perpendicularly with the quartz tube axis. The temperature profiles of the burning particles were obtained by taking several readings along the axis of quartz tube. Radiations from the burning particles were detected by the pyrometer and then processed by a computer software called SensorTools. Table 4 shows the DTF test conditions during all the experiments.

Parameter	Value
Temperature	1373 K
Airflow	1 L/min
Air pressure	1 bar

Table 4: DTF test conditions.

3.3. Two-color pyrometer

A two-color *SensorTherm GMBH* pyrometer was used to undertake the temperature measurements. It was placed on a vertically movable stand to get the temperature profiles along the axis of the quartz tube. The distance between the DTF and pyrometer was kept minimum (~340-360mm) since it provided the smallest focus point of 0.8 mm that enabled us to capture the radiations from the smaller fuel particles [24]. The pyrometer had the effective wavelengths of 0.7 and 1.1 µm. The measurements were done starting from a distance of 10 cm from the injector tip till 15 cm in downward direction. The reason for

choosing this distance range was that the pyrometer could not catch the significant radiation before that distance because the particle velocity was too high to be captured by the pyrometer. Also, due to airflow of 1 L/min, particles were carried away from the injector tip quite swiftly making it difficult for the pyrometer to get a stable reading.

Table 5 shows the pyrometer parameters used.

Parameter	Value
Measurement distance	340 - 360 mm
Emissivity ratio	1.00 – 1.40
Spot size	~0.8 mm
Buffer interval	2, 16 ms

Table 5: Pyrometer parameter used.

Figure 12 shows the experimental setup of pyrometer on the moveable stand that allowed to measure the temperature profiles along the quartz tube axis through the viewing window.

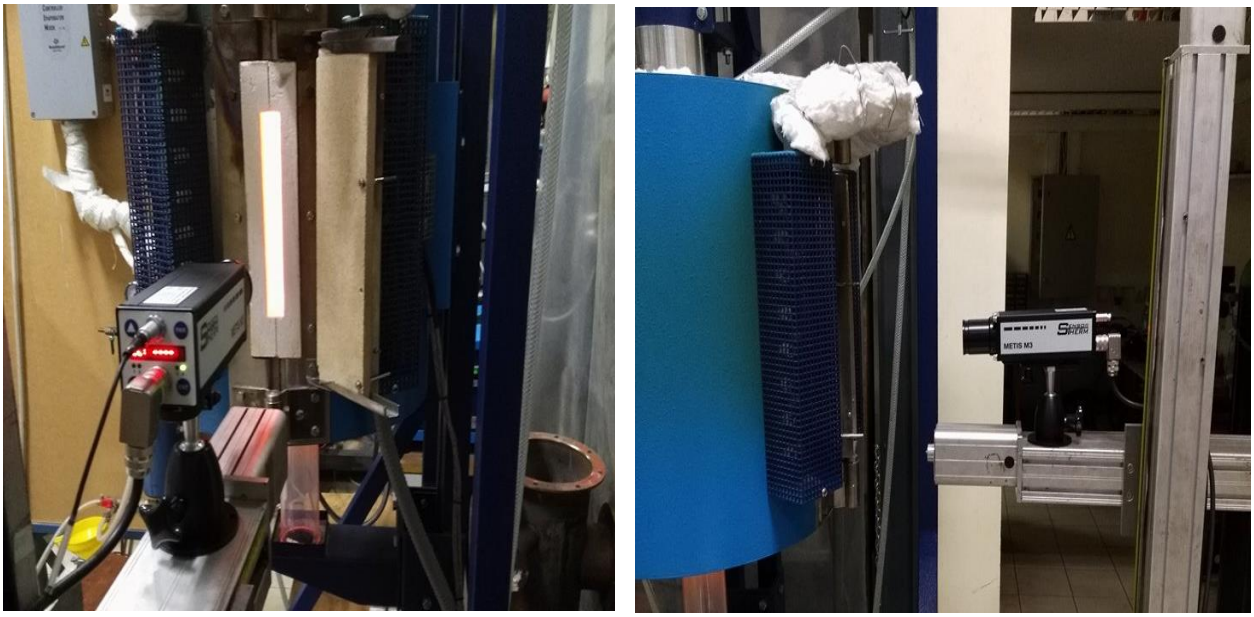

Back view **Side View**

Figure 12: Side and back views of pyrometer setup.

As described in pyrometer manual [24], the emissivity values of the fuel particles can be ruled out if the radiation signals on two wavelengths are parallel to each other (see Figure 13) thereby minimizing the uncertainty in the measurements. Figure 14 indicates that in the present experiments, the temperature

values at both the wavelengths were parallel to each other. Hence, the particles emissivity was not considered in the calculations.

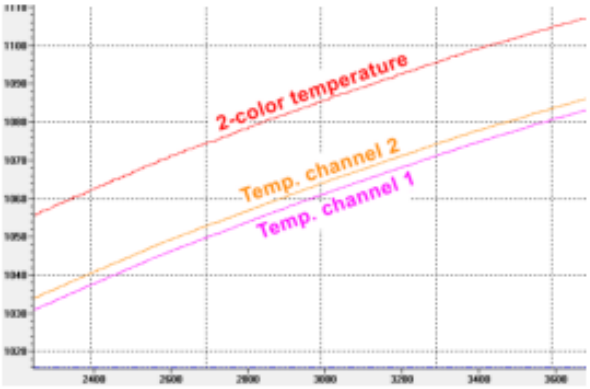

Figure 13: 1 - Color and 2 - Color results comparison [24].

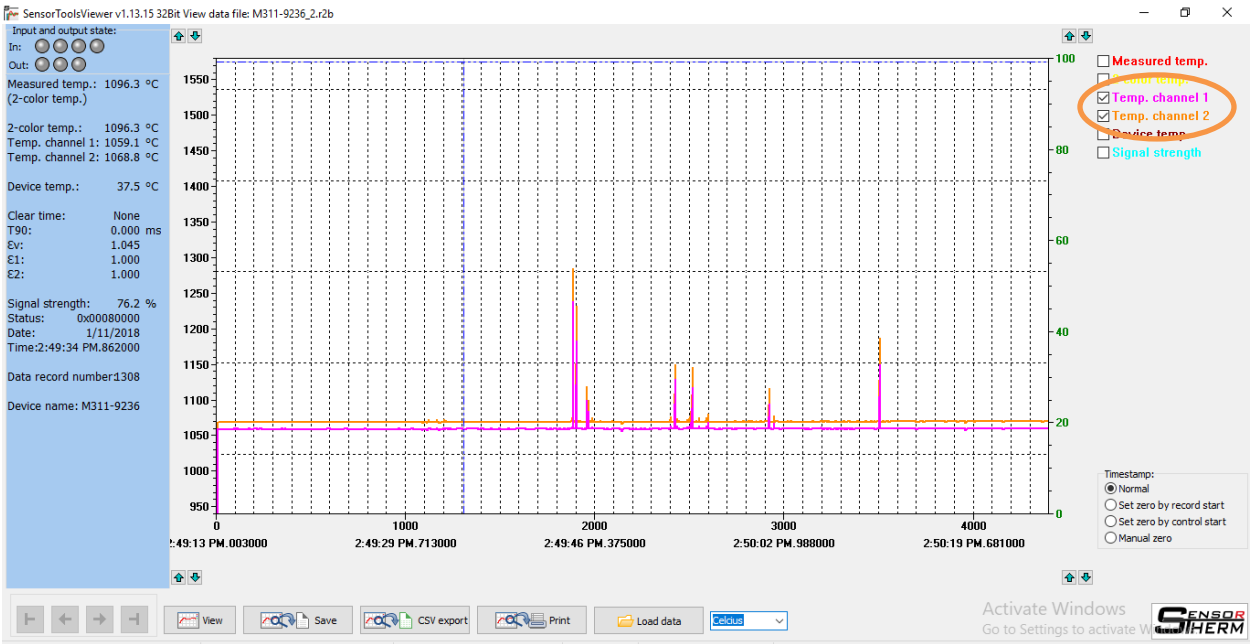

Figure 14: Solid fuel temperature at two wavelengths.

3.3.1. SensorTools software

This software connects the pyrometer with the computer and gives a direct temperature value of the object under consideration. The pyrometer is connected to the computer and it can be defined with the software either to operate it in 1 - color or 2 - color mode. In all the measurements, the 2 - color mode was chosen since it provides better results due to less uncertainties in emissivity variations.

So, after setting up the pyrometer and connecting it with the software, the parameters were set up as mentioned in table 3 and it was ready to go. The software provides the flexibility to use the pyrometer at numerous values of different parameters such as emissivity ratio, number of wavelengths, buffer rates, spot size etc.

The emissivity ratio used in the experiments ranges from 1.00 to 1.40 depending on the optical clarity/transmittance of the quartz tube. For a relatively clear, transparent and shiny tube, which was used in the latter half of the experiments, the DTF temperature measured by the two thermocouples was the same as that calculated by the pyrometer for an emissivity ratio of 1.00, so there was no need to change it. However, in the initial experiments, the thermocouples readings did not match the pyrometer readings due the relatively inferior optics of the old quartz tube, so that a higher emissivity ratio of 1.40 was used.

The buffer rate is the parameter that controls the number of readings taken by the pyrometer per second. As it can be seen from the Table 5, two buffer rates were used in the experiments. In the first half of the experiments, a buffer rate of 16 ms was used, but then it was realized that there was a possibility of missing many particle readings as they passed by the pyrometer so fast that it could not catch the radiation signal. So, after few trials, a value of 2 ms was used, which significantly improved the pyrometer measurements.

3.3.2. ArcSoft showbiz software

This software was used to record the videos captured by the pyrometer. After connecting the pyrometer, this software was opened along with SensorTools. It also served the purpose of adjusting the focus of the pyrometer.

3.3.3. Post processing of data

The *SensorTools* software provides the results in the form of graphs as shown in Figure 15.

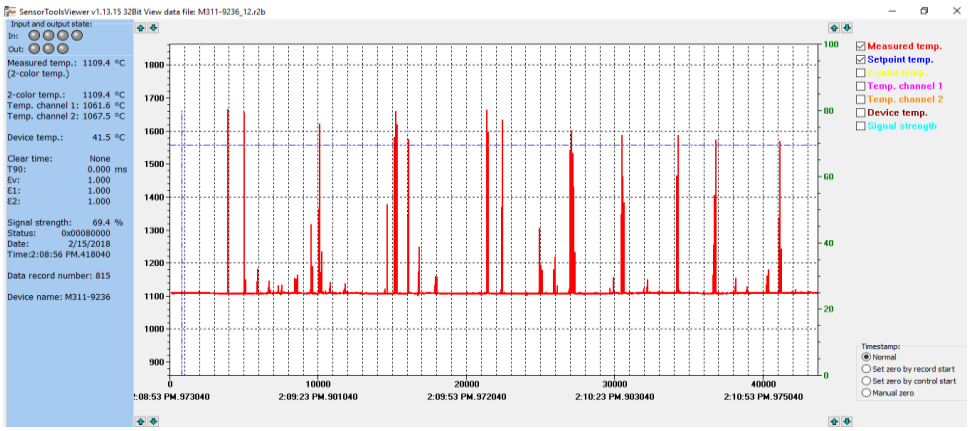

Figure 15: Output graphs of the SensorTools software.

The post processing of the data was done by exporting the graph to an Excel file that provided the temperature values for each millisecond. The excel file also included the signal strength of the pyrometer for each millisecond. It was established after detailed consultation with the pyrometer supplier that the signal strength can be a good criterion for selecting the true particle temperature. As the signal strength ranges from 0 to 100% depending on the radiation received by the pyrometer sensor, it was explained by the supplier that this signal strength depends on the surface area and density of the radiation emitting object. When there was no particle, the signal strength was maximum as pyrometer was focused on the DTF walls, which were at 1373 K, but on passing the particle on the pyrometer focus point, signal strength dropped to values ranging from 10-40%. The reason for such low particle signal strength as compared to signals from the DTF walls is that the particles have lower surface area and density thereby producing weaker signals. So, it was thought out that this phenomenon can serve as a good criterion for choosing the true temperature values and therefore, all the peak temperature values whose signal strength lies in between 10-40% were selected to calculate the mean particle temperature.

Furthermore, the temperature readings were taken at 6 different distances starting from 10 cm till 15 cm from the injector tip to obtain the temperature profiles of fuel particles along the axis of the quartz tube. So, the above discussed procedure was applied to all the readings to get the mean particle temperature at different heights.

3.4. Uncertainties in measurements

The major uncertainty faced during the experiments was the accuracy of the measured radiation signals when a fuel particle passed through the focus point of the pyrometer. It was established that particles do not always pass exactly at the center of the focus point owing to their direction when they leave the injector. Although an air flow distributor was also used to straight the flow inside the quartz tube, there were still some turbulences that hindered the particles to have a perfect flow direction.

4. RESULTS AND DISCUSSION

4.1. Gas temperature

In all experiments, the fuel particles were combusted in air (21% O_2/79% N_2). The gas temperature in the heated quartz tube with a DTF wall temperature of 1373 K was measured with Pt-Rh thermocouples. The temperature of the air was measured at the same distances from the injector tip at which particle temperature was measured. Figure 16 shows the gas temperature profile along the axis of quartz tube.

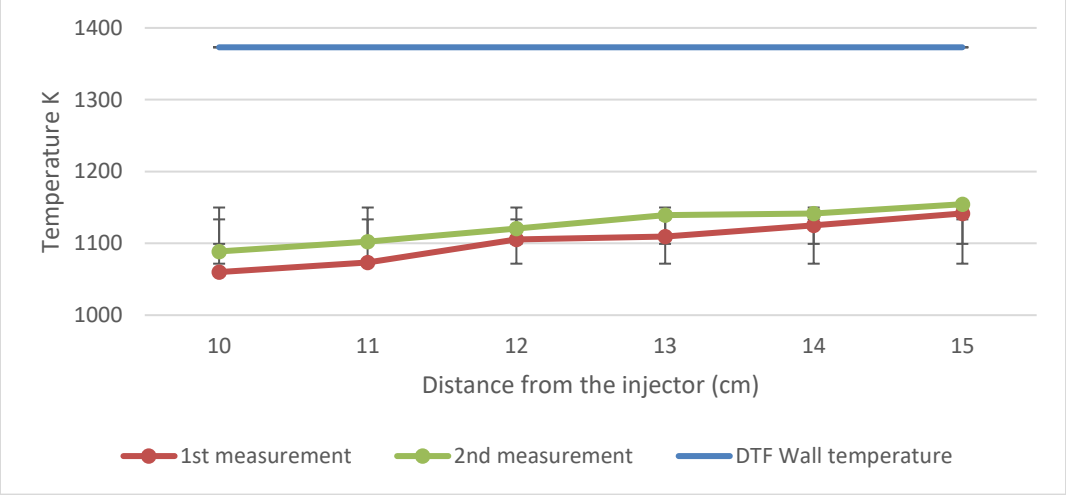

Figure 16: Gas temperatures in DTF.

The measurements were repeated twice to verify the results. In both the cases, it is evident that the temperature of the air increased as the distance to the injector tip increased. This trend was similar to that observed by Khatami [8] and Riaza [14], as shown in Figure 17.

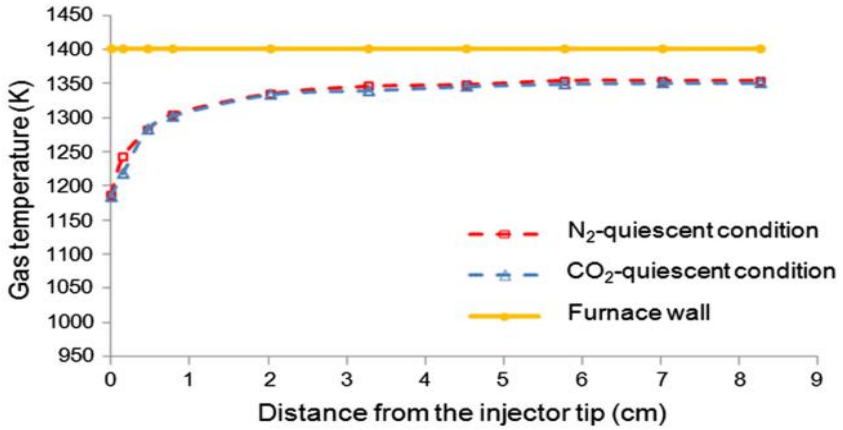

Figure 17: Centerline gas temperature inside the drop-tube furnace [14].

4.2. Bituminous coal particle temperature

Mean particle temperature of Brazilian bituminous coal particles with size below 150 µm was measured using the pyrometer using the method described in chapter 3. Figure 18 shows the particle measurements for two different pyrometer settings. In the "1st measurement", a buffer rate of 16 ms was used and, as mentioned before, there was the possibility of skipping many particles as they passed through the focal point of pyrometer and hence, affecting the final measurements. After discussing with the pyrometer supplier, it was decided that the buffer rate should be decreased to 2 ms that would increase the number of readings taken by the pyrometer per second. The experiment was repeated with this new parameter and it can be seen in 2nd measurement that there was improvement in the results.

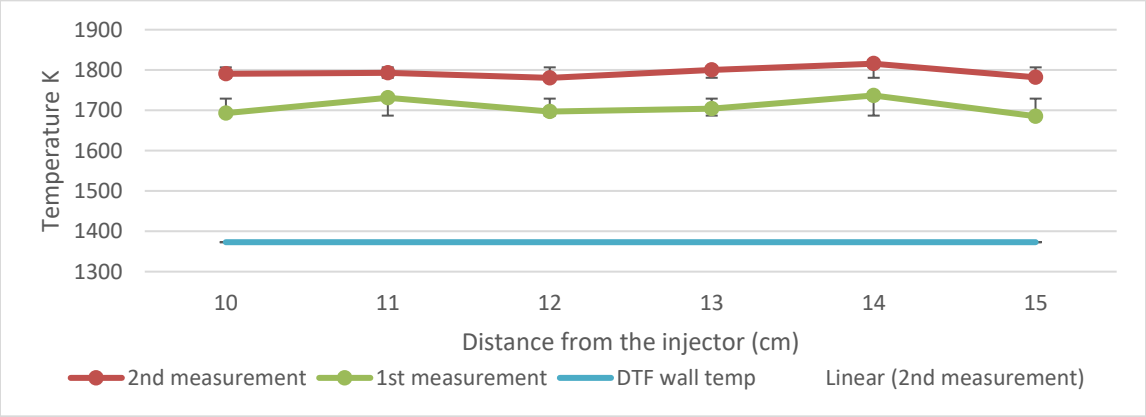

Figure 18: Mean particle temperature of bituminous coal particles.

The temperature range observed in these experiments for bituminous coal is in close agreement with the temperature range obtained by Levendis [9] and Riaza [14]. Figure 19 and 20 show the results obtained by Riaza and Levendis, respectively, for the combustion of a bituminous coal in air at a DTF wall temperature of 1400 K. They used a bituminous coal of 90 µm at a DTF wall temperatures of 1400 K and their results showed temperature in the range 1600-1800 K which is in close agreement with the present results.

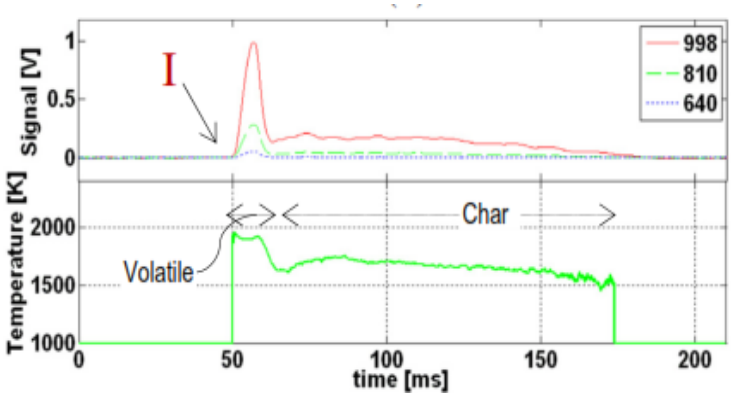

Figure 19: Temperature of bituminous coal particles (75–150 µm) [14].

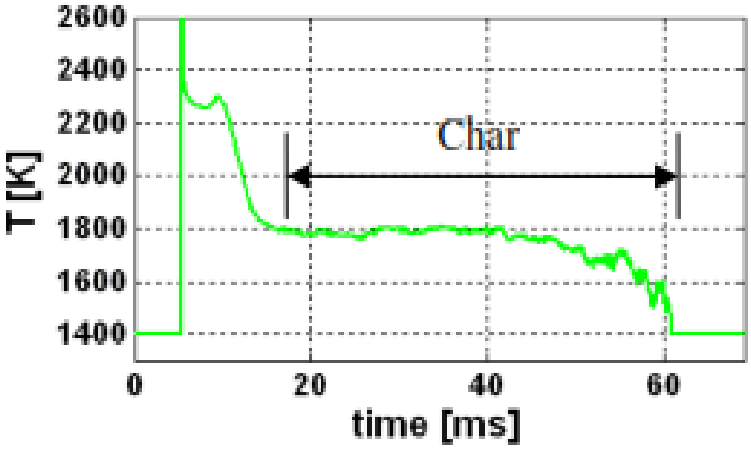

Figure 20: Temperature of bituminous coal particles (75–90 µm) [9].

The peak temperature at the start of these graphs obtained by Riaza and Levendis is the ignition temperature which is not measured in our results. The reason is that in this study, the particles were started to be monitored after a distance of 10 cm from injector tip at which the particles were already ignited and secondly, they were not monitored from the top side along the axis of quartz tube like other studies, rather they were monitored horizontally because measurement of ignition temperature was out of scope for this study.

4.3. Wheat straw particle temperature

The Portuguese wheat straw biomass with a particle size in between 150-200 µm was burned in the drop-tube furnace and the temperature was measured using the pyrometer. During all these measurements with biomass, the buffer rate was kept at 2 ms to get the maximum number of temperature readings per

second, which as it was seen in the previous experiments with bituminous coal, improved the results significantly. Figure 21 shows the results obtained from this experiment.

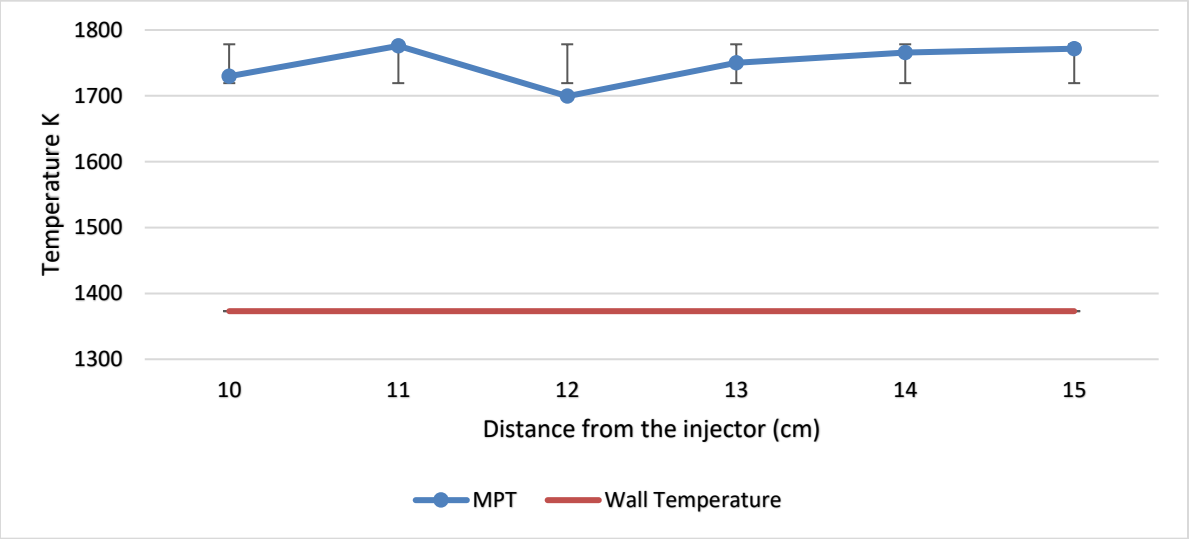

Figure 21: Mean particle temperature of wheat straw biomass (150-200 µm).

The temperature range of Portuguese wheat straw is quite similar to that obtained in the case of Brazilian bituminous coal as evident from Figure 22.

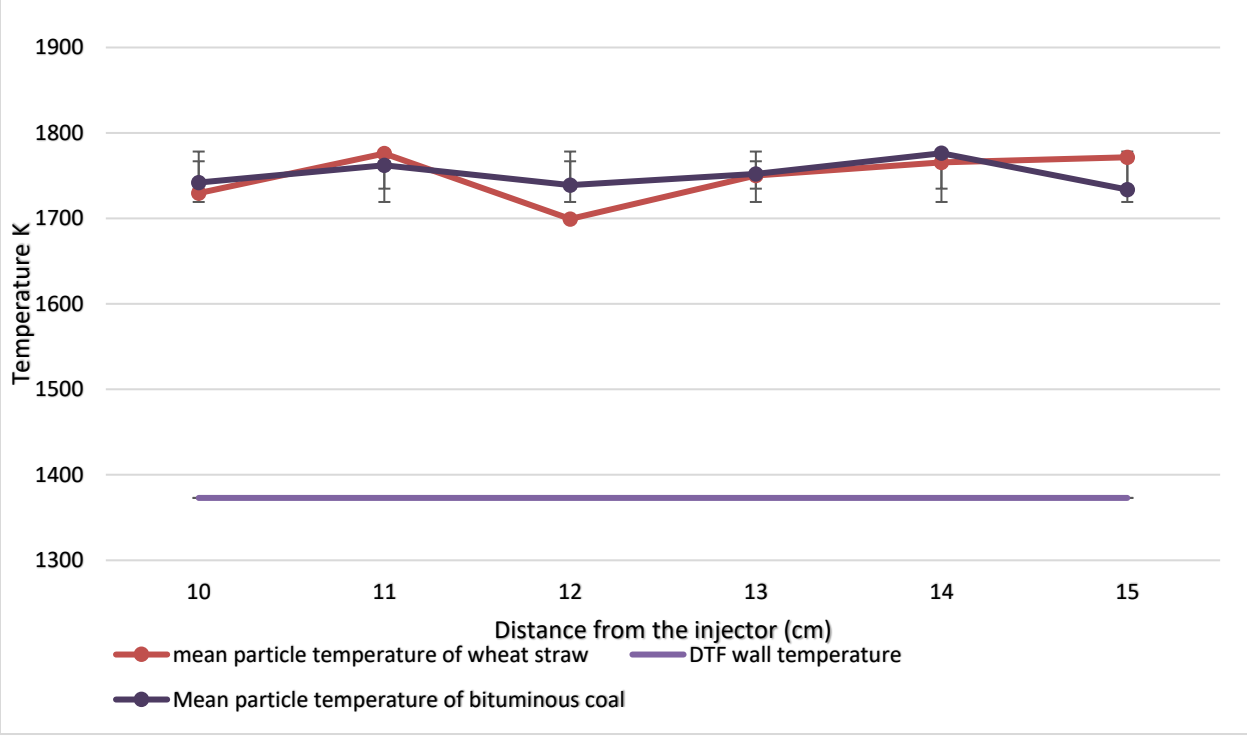

Figure 22: Temperature comparison of bituminous coal and wheat straw.

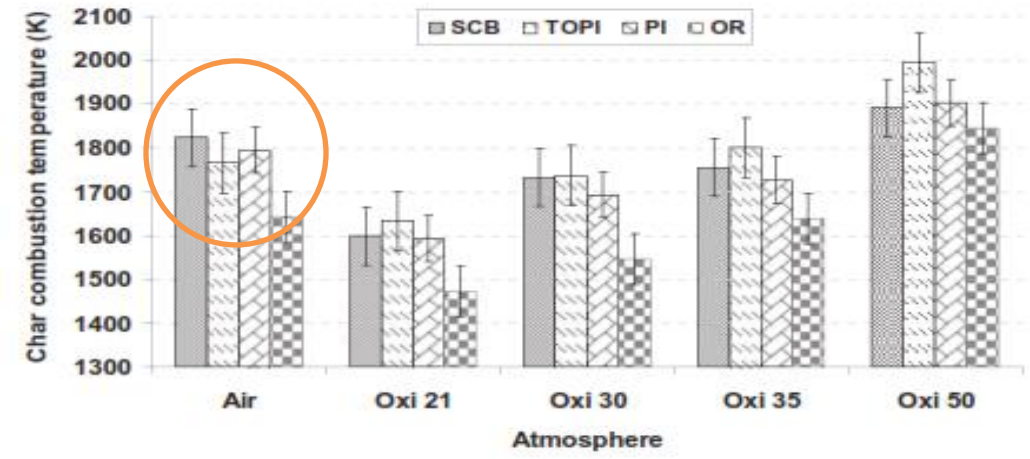

OR	Olive residue
SCB	Sugarcane bagasse
PI	Pine sawdust
TOPI	Torrefied pine sawdust

Figure 23: Temperature profiles of different biomasses under different conditions [9].

Figure 23 shows the results obtained by Khatami and Levendis using a three-color pyrometry. It can be seen that for all types of biomass fuels used, the single particle temperature for combustion in air lies in the range of 1700-1800 K, which endorses the test results obtained in this work.

4.4. Critical assessment of the temperature measurements

One of the main hurdles in carrying out these experiments was the optical quality of the quartz tube as it was one of the main factors in measuring the temperature by pyrometer. The pyrometer measures the radiation from the hot object to produce a temperature value. The incoming radiation is greatly affected by the optical properties of the quartz tube that comes in between the particle and pyrometric lens. Its transmittance and clarity affect the radiation passing through it and ultimately the temperature readings. With the frequent use of the quartz tube at a high temperature of 1373 K, it started getting cloudy thereby restricting the optical access of the pyrometer to the particles and ultimately, compelling the experiments to be stopped completely at one point until the tube was replaced by a new one. Figure 24 shows the damaged quartz tube.

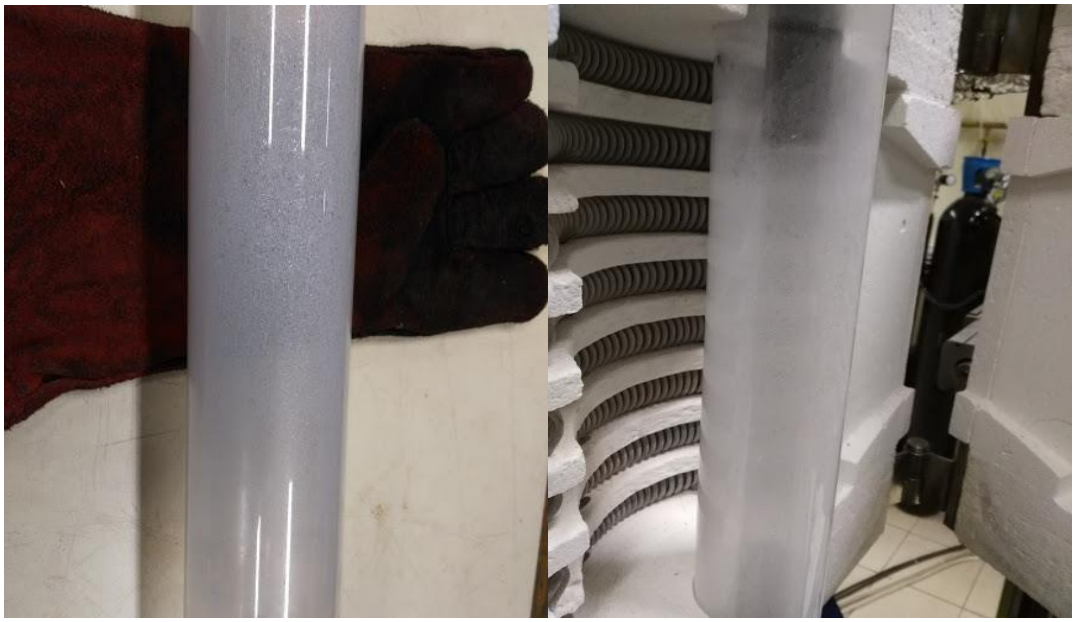

Figure 24: Damaged quartz tube.

5. CLOSURE

5.1. Conclusions

In this work, a two-color pyrometer was used to measure the single particle temperature of two fuels: a Brazilian bituminous coal with a particle size below 150 μm and a Portuguese wheat straw with particle size in the range 150-200 μm. The combustion environment was air with a flowrate of 1 L/min and 1 bar pressure. The particles were introduced through the injector with the help of a syringe needle from the top of a DTF. The DTF, electrically heated at 1373 K, was provided with an 82 cm long quartz tube with radiation cavity of 30 cm. Two windows were available sideways for optical access that were used for pyrometric measurements. Measurements were taken at a distance of 10-15 cm from the injector tip in each case to obtain temperature profiles for the solid fuel burning particles. The results can be summarized as follows:

- In both the cases with bituminous coal and wheat straw, the temperature profiles of particles obtained were comparable to previous studies.
- Both the bituminous coal particles and wheat straw particles burned in a temperature range of 1700-1800 K in air environment.
- The results obtained seem to be satisfactory and this method can be used further to measure particle temperatures of more solid fuels.

5.2. Future work

This particular work established the method of pyrometric measurements of solid fuels particle temperatures along the axis of a DTF. Now more solid fuels can be studied. Furthermore, this same study can also be repeated by changing the combustion environments such as oxy-fuel conditions to compare the results with previous studies.

REFRENCES

[1] BP, “BP Energy Outlook Energy 2017,” *BP Stat. Rev. World Energy*, p. 52, 2017.

[2] BP, “Statistical Review of World Energy,” *BP Stat. Rev. World Energy*, no. June, pp. 1–48, 2016.

[3] R. Saidur, E. A. Abdelaziz, A. Demirbas, M. S. Hossain, and S. Mekhilef, “A review on biomass as a fuel for boilers,” *Renew. Sustain. Energy Rev.*, vol. 15, no. 5, pp. 2262–2289, 2011.

[4] J. Koppejan, L. Baxter, “Global operational status on cofiring biomass and waste with coal Experience with different cofiring concepts and fuels,” Biomass, vol. 2, pp. 1–14, 2013.

[5] H. Haykiri-Acma, A. Z. Turan, S. Yaman, and S. Kucukbayrak, “Controlling the excess heat from oxy-combustion of coal by blending with biomass,” *Fuel Process. Technol.*, vol. 91, no. 11, pp. 1569–1575, 2010.

[6] T. Joutsenoja, P. Heino, R. Hernberg, and B. Bonn, “Pyrometric temperature and size measurements of burning coal particles in a fluidized bed combustion reactor,” *Combust. Flame*, vol. 118, no. 4, pp. 707–717, 1999.

[7] J. Riaza, J. Gibbins, and H. Chalmers, “Ignition and combustion of single particles of coal and biomass,” *Fuel*, vol. 202, pp. 650–655, 2017.

[8] R. Khatami, C. Stivers, K. Joshi, Y. A. Levendis, and A. F. Sarofim, “Combustion behavior of single particles from three different coal ranks and from sugar cane bagasse in O_2/N_2 and O_2/CO_2 atmospheres,” *Combust. Flame*, vol. 159, no. 3, pp. 1253–1271, 2012.

[9] J. Riaza *et al.*, “Combustion of single biomass particles in air and in oxy-fuel conditions,” *Biomass and Bioenergy*, vol. 64, pp. 162–174, 2014.

[10] M. Rodriguez, R. Raiko, “Effect of O_2 and CO_2 content on particle surface temperature and size of coal char during combustion,” no. January, pp. 28–29, 2009.

[11] L. D. Timothy, A. F. Sarofim, “Characteristics of single particle coal combustion," Department of Chemical Engineering , in *International combustion symposium*, 1982.

[12] D. J. Maloney, E. R. Monazam, S. D. Woodruff, L. Lawson, and W. Virginia, “Temperature measurements of single coal particles during the early stages of heating and devolatilization,” vol. 84, no. 1–2, pp. 721–729, 1991.

[13] P. A. Bejarano, Y. A. Levendis, “Single coal particle combustion in $O_2/N_2$and O_2/CO_2 environments,” *Combust. Flame*, vol. 153, no. 1–2, pp. 270–287, 2008.

[14] J. Riaza *et al.*, “Single particle ignition and combustion of anthracite, semi-anthracite and bituminous coals in air and simulated oxy-fuel conditions,” *Combust. Flame*, vol. 161, no. 4, pp. 1096–1108, 2014.

[15] X. Shen, “Coal combustion and combustion products,” *Encycl. Life Support Syst.*, vol. I, pp. 2–8, 2002.

[16] P. Coelho, M. Costa, *Combustão*, 2a edition, ORION,2012.

[17] G. Simões, "Single particle ignition of pulverized solid biomass fuels : experiments and modeling," MSc Thesis, Instituto Superior Tecnico, 2016.

[18] S. Vassilev, D. Baxter, "An overview of the chemical composition of biomass," *Fuel*, vol. 89, pp. 913–933, 2010.

[19] M. Asadieraghi, W. M. A. Wan Daud, "Characterization of lignocellulosic biomass thermal degradation and physiochemical structure: Effects of demineralization by diverse acid solutions," *Energy Convers. Manag.*, vol. 82, pp. 71–82, 2014.

[20] H. Yang, R. Yan, H. Chen, D. H. Lee, and C. Zheng, "Characteristics of hemicellulose, cellulose and lignin pyrolysis," *Fuel*, vol. 86, no. 12–13, pp. 1781–1788, 2007.

[21] P. McKendry, "Energy production from biomass (part 1): overview of biomass," *Bioresour. Technol*, vol. 83, no. 1, pp. 37–46, 2002.

[22] R. Khatami, Y. A. Levendis, "On the deduction of single coal particle combustion temperature from three-color optical pyrometry," *Combust. Flame*, vol. 158, no. 9, pp. 1822–1836, 2011.

[23] IMPAC Infrared GMBH, "Pyrometer- Handbook," p. 35, 1999.

[24] M. Studios, A. R. Reserved, *User Manual*, no. September. 2010.

[25] J. Maron, "Selecting non contact pyrometers & infrared thermometers," *Process Heating Magazine*, vol. 9, pp. 1–7, 1999.

[26] L. L. Baxter, T. H. Fletcher, and D. K. Ottesen, "Spectral emittance measurements of coal particles," *Energy & Fuels*, vol. 2, no. 4, pp. 423–430, 1988.

[27] V. Branco, M. Costa, "Effect of particle size on the burnout and emissions of particulate matter from the combustion of pulverized agricultural residues in a drop tube furnace," *Energy Convers. Manag.*, vol. 149, pp. 774–780, 2017.

[28] R. B. Kops, F. M. Pereira, M. Rabaçal, and M. Costa, "Effect of steam on the single particle ignition of solid fuels in a drop tube furnace under air and simulated oxy-fuel conditions," accepted for presentation at *37th International Symposium on Combustion*, 2018.